Reverse Osmosis Network Rigorous Design Optimization

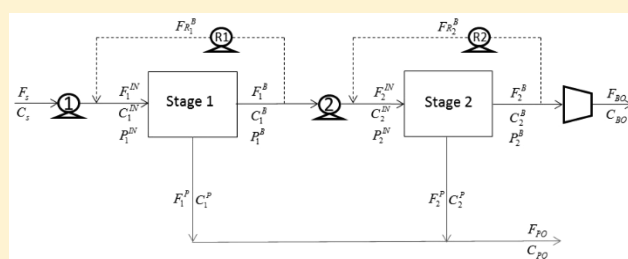Abdon Parra,[†] Mario Noriega,[‡] Lidia Yokohama,[†] and Miguel Bagajewicz*,[§]

[†]Departamento de Processos Inorgânicos, Escola de Química, Universidade Federal de Rio de Janeiro, Rio de Janeiro, 21941-901, Brazil

[‡]Departamento de Ingeniería Química y Ambiental, Universidad Nacional de Colombia, Bogotá, Colombia

[§]School of Chemical Engineering and Material Science, University of Oklahoma, 100 East Boyd Street, T-335, Norman, Oklahoma 73019-0628, United States

Ⓢ *Supporting Information*

ABSTRACT: In this work, we propose a methodology to solve a nonlinear mathematical model for the optimal design of reverse osmosis (RO) networks, which ameliorates the shortcomings of the computational performance and sometimes convergence failures of commercial software to solve the rigorous mixed integer nonlinear programming (MINLP) models. Our strategy consists of the use of a genetic algorithm to obtain initial values for a full nonlinear MINLP model. In addition, because the genetic algorithm based on the rigorous model equations is insurmountably slow, we use metamodels to reduce the mathematical complexity and considerably speed up the run. We explore the effects of the feed flow, seawater concentration, number of reverse osmosis stages, and the maximum number of membrane modules in each pressure vessel on the total annualized cost of the plant.

1. INTRODUCTION

The increased demand for fresh water by a growing population and the per capita increase in the demand for fresh water due to industrialization and urbanization makes desalination a competitive technology for the generation of pure water from seawater as well as other low-quality water containing salts and other dissolved solids.[1]

The available desalination technologies in the market can be classified as thermal-based and membrane-based processes. Reverse osmosis (RO), multistage flash (MSF), and multieffect distillation (MED) are the main commercial desalination technologies, with RO being the fastest growing.[2] This last technology (RO) is, in most cases, the technology of choice for seawater desalination in places where inexpensive waste heat is not available.

Desalination plants using RO have been traditionally designed by manufacturers using empirical approaches and heuristics.[3] However, the cost performance of RO desalination is sensitive to the design parameters and operating conditions,[4] and therefore, attention needs to be focused on obtaining cost-optimal designs.

The problem of synthesizing a reverse osmosis network (RON) consists of obtaining a cost-effective solution based on optimum values of the following: number of stages, number of pressure vessels per stage, number of modules per pressure vessel, number and type of auxiliary equipment, and the operational variables for all the devices of the network.

After the early works of Evangelista,[5] El-Halwagi et al.,[6] and Voros et al.,[7,8] many papers have followed,[9−15] mainly using the

solution-diffusion model proposed by Al-Bastaki et al.,[16] a model that includes the effect of concentration polarization, which eliminates the problem of significant overestimation of the total recovery,[17] and the economic model from Malek et al.[18]

Many authors proposed solving the problem of the design of a RON using mixed integer nonlinear programming (MINLP) or nonlinear programming (NLP).[3] For example, Du et al.[19] used a two-stage superstructure representation and solved the resulting MINLP using the solvers CPLEX/MINOS using several starting points to obtain the best solution. They do not clarify how they generated these starting points. Sassi and Mujtaba[20] proposed a MINLP model and solved the problem using an outer approximation algorithm within gPROMS to evaluate the effects of temperature and salt concentration in the feed current. They do that by generating "various structures and design alternatives that are all candidates for a feasible and optimal solution", without specifying how their initial values are obtained. Alnouri and Linke[21] explored different specific RON structures, and they optimized each using the "what's Best" Mixed-Integer Global Solver for Microsoft Excel by LINDO Systems Inc. The solver is global and does not require initial points. They used "reduced super-structures resembling fundamentally distinct design classes".
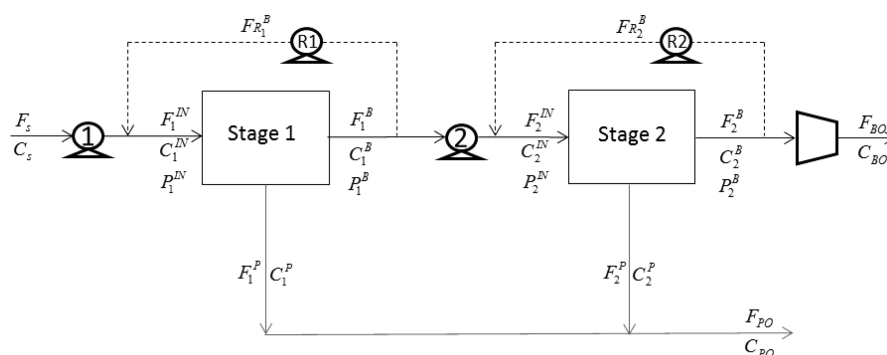
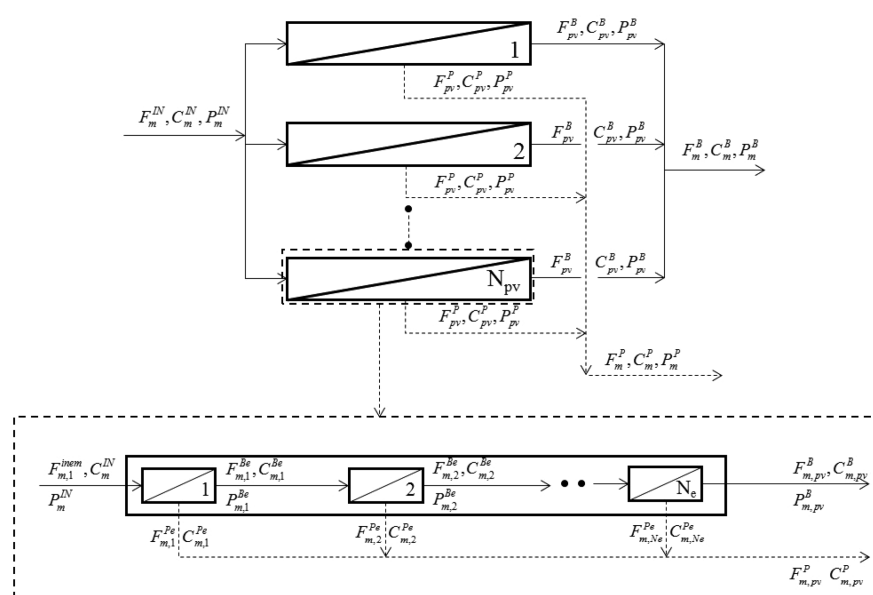**Figure 1.** Superstructure of a two-unit reverse osmosis network.

Figure 2. Structure of a single stage.

Lu et al.[22] obtained an optimal RON using a two-stage RON structure and used an MINLP technique with several starting points obtained from an ad hoc preliminary simulation. Finally, Skiborowski et al.[23] proposed an optimization strategy with a special initialization scheme where a feasible initial solution is obtained in two steps: first, all variables are initialized with reasonable values (some obtained by heuristics) and then a solution is obtained using SBB and SNOPT solvers. These local minima are reportedly obtained within a few minutes of computation. They also reported an attempt to solve a RON using the global solver Baron, indicating that the solver finished after 240 h with a relative gap of 15.66%.

All the aforementioned works have a few things in common: they share the complexity of the problem modeling and the difficulty of the solution procedure that stem from the nonlinearities associated with the concentration polarization model. In some cases, they do not indicate in detail what preprocessing was done and how they obtained the initial data and/or the computing time. Regarding computing time, it varies: 1 min to a few minutes,[23] 3−16 min,[10] or 5−28 h.[19] Our experience indicates that, without the initial values, there is no convergence in several solvers. In addition, although computational time is not critical in design procedures, we believe it ought to be reasonable. In some cases, the computational time is unacceptable,[19] as it is on the order of

days. In this article, we intend to ameliorate these short-comings providing these initial data systematically, and reducing the computing time to the order of minutes.

To aid in our work, we also use surrogate models, often called "metamodels", which have been proposed to address the issue of model complexity and the associated difficulties of convergence when poor or no initial points are given. Such metamodels are sets of equations of simple structure (low-order polynomial regression, and Kriging or Gaussian process[24]) that facilitate an increased computational performance (mostly time[25]). They are built with the information on the rigorous method, and their functions approximate well the image of the more complicated models.[26] Metamodels were implemented in the optimization for a heat exchanger network,[27,28] the optimization of water infrastructure planning,[29,30] in stochastic structural optimization,[31] and in building energy performance.[32]

In this work, the RON optimization problem is formulated as an MINLP problem that minimizes the total annualized cost (TAC). The model is first solved using a genetic algorithm, which provides good initial values for the rigorous MINLP model. As we shall observe, a genetic algorithm, using the full nonlinear and rigorous equations, is computationally very expensive, while the MINLP is rather fast when good initial values are provided. We will show that replacing the use of
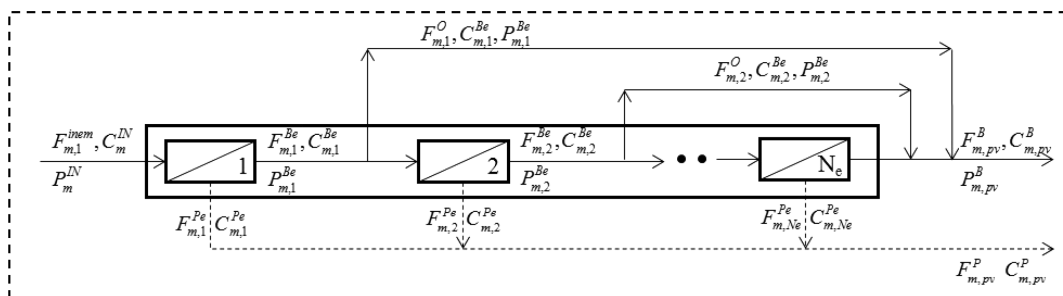
Figure 3. Bypass representation of a single pressure vessel.

rigorous equations of the model by the use of a metamodel in the genetic algorithm speeds up the solution time orders of magnitude and provides a similar solution.

2. MATHEMATICAL MODEL

Figure 1 presents a reverse osmosis network involving two stages, pumps, and turbines. Each stage consists of a set of parallel pressure vessels. Figure 1 also presents the brine recycles for each stage. Figure 2, in turn, presents the structure of a stage and the membrane modules in series.

The feed flow enters a high-pressure pump and is sent to the first RO stage, where it is separated into two streams: permeate and brine. The brine leaving the first RO stage feeds the second RO stage, but a fraction could be recycled. Recycling increases the velocity through the membrane module and thus reduces the concentration polarization. The final brine from the second stage goes to a turbine to recover the residual energy. The permeates from stages 1 and 2 are mixed to get the final permeate.

In this work, we consider spiral wound (SW) modules because of their high packing density and relatively low energy consumption. Thus, a diffusion model for spiral wound (SW) modules with FilmTec SW30HR-380 membrane modules is used.

Rigorous MINLP Model. We now show the equations of a rigorous MINLP model.

global balances:

$$F_S = \hat{F}_{PO} + F_{BO} \tag{1}$$

$$F_S C_S = \hat{F}_{PO} C_{PO} + F_{BO} C_{BO} \tag{2}$$

recycle balances:

$$F_1^{IN} = F_S + F_{R_1}^B \tag{3}$$

$$F_1^{IN} C_1^{IN} = F_S C_S + F_{R_1}^B C_1^B \tag{4}$$

$$F_2^{IN} = F_1^B - F_{R_1}^B + F_{R_2}^B \tag{5}$$

$$F_2^{IN} C_2^{IN} = F_1^B C_1^B - F_{R_1}^B C_1^B + F_{R_2}^B C_2^B \tag{6}$$

balances for outlet permeate stream:

$$\hat{F}_{PO} = \sum_{m=1}^{N_{RO}} F_m^P \tag{7}$$

$$\hat{F}_{PO} C_{PO} = \sum_{m=1}^{N_{RO}} F_m^P C_m^P \tag{8}$$

$$C_{PO} \leq C_P^{max} \tag{9}$$

balances for outlet brine stream:

$$F_{BO} = \sum_{m=1}^{N_{RO}} F_m^{B-F_{BO}} + \sum_{t=1}^{N_T} F_t^{T-F_{BO}} \tag{10}$$

$$F_{BO} C_{BO} = \sum_{m=1}^{N_{RO}} F_m^{B-F_{BO}} C_m^B + \sum_{t=1}^{N_T} F_t^{T-F_{BO}} C_t^T \tag{11}$$

Reverse Osmosis Stages Model. The feed of the RO stage is distributed equally to the N_{pv} pressure vessels of each stage:

$$F_m^{inem} N_{pv_m} = F_m^{IN} \tag{12}$$

We decided to make this a continuous variable to reduce the computation complexity, and the approximate result will be obtained by rounding the variable. Other authors also use the same concept, except Du et al.,[19] who used binaries to model the number of pressure vessels.

The inlet flow of a membrane module its restricted to a specific range by the commercial provider:

$$F_m^{minin} N_{pv_m} \leq F_m^{IN} \leq F_m^{maxin} N_{pv_m} \tag{13}$$

For the remaining $e = 2, ..., N_e$ modules within each pressure vessel, the incoming properties are equal to those of the brine of the previous module, so the properties of the brine final current are obtained from the last series module.

first module:

$$F_{m,1}^{Be} = F_m^{inem} - F_{m,1}^{Pe} \tag{14}$$

$$F_{m,1}^{Be} C_{m,1}^{Be} = F_m^{inem} C_m^{IN} - F_{m,1}^{Pe} C_{m,1}^{Pe} \tag{15}$$

rest of the modules:

$$F_{m,e}^{Be} = F_{m,e-1}^{Be} - F_{m,e}^{Pe}, \qquad \forall\, e \neq 1 \tag{16}$$

$$F_{m,e}^{Be} C_{m,e}^{Be} = F_{m,e-1}^{Be} C_{m,e-1}^{Be} - F_{m,e}^{Pe} C_{m,e}^{Pe}, \qquad \forall\, e \neq 1 \tag{17}$$

The final brine current of the corresponding RO stage is obtained from

$$F_m^B = N_{pv_m} F_{m,N_e}^{Be} \tag{18}$$

$$C_m^B = C_{m,N_e}^{Be} \tag{19}$$

$$P_m^B = P_{m,N_e}^{Be} \tag{20}$$

The flow of the permeate current is obtained from the mass and component balances of the hole stage as follows:

$$F_m^P = F_m^{IN} - F_m^B \tag{21}$$

$$F_m^P C_m^P = F_m^{IN} C_m^{IN} - F_m^B C_m^B \tag{22}$$

In practice, the modules inside the pressure vessel are all connected in series. However, to be able to consider a variable number of pressure vessels, we consider the maximum number and add splits to remove some flow rate $F_{m,e}^O$ from each module (Figure 3) out of a total fixed number of pressure vessels. The optimization determines the optimal number and will bypass the rest.

To model these bypasses, we introduce binary variables $y_{m,e}^O$ which are 1 if a flow $F_{m,e}^O > 0$, and 0 otherwise. Thus, we introduce the following equations:

$$F_{m,e}^O - \Gamma y_{m,e}^O \le 0 \tag{23}$$

We force that only one of the flows is different from zero, writing

$$\sum_{e=1}^{N_e} y_{m,e}^O = 1 \tag{24}$$

In addition, to make sure that $F_{m,e}^{Be} = F_{m,e}^O$ when $y_{m,e}^O = 1$, we write

$$(F_{m,e}^{Be} - F_{m,e}^O) - \Gamma(1 - y_{m,e}^O) \le 0 \tag{25}$$

To obtain the number of modules N_e in a pressure vessel, we use the next expression:

$$N_{em} = 1y_{m,1}^O + 2y_{m,2}^O + 3y_{m,3}^O + 4y_{m,4}^O + 5y_{m,5}^O + 6y_{m,6}^O + 7y_{m,7}^O + 8y_{m,8}^O \tag{26}$$

Diffusion Membrane Model. The flux for water $J_{m,e}^w$ for one membrane module is given by the following equations:

$$J_{m,e}^w = \hat{a}\Delta P_{m,e}^{nd} \tag{27}$$

where $\hat{a}$ is the pure water permeability, with the net driving pressure difference given by

$$\Delta P_{m,1}^{nd} = P_m^{IN} - \frac{\Delta P_{m,1}^B}{2} - \hat{P}_{m,1}^{Pe} - (\pi_{m,1}^W - \pi_{m,1}^P) \tag{28}$$

$$\Delta P_{m,e}^{nd} = P_{m,e-1}^{Be} - \frac{\Delta P_{m,e}^B}{2} - \hat{P}_{m,e}^{Pe} - (\pi_{m,e}^W - \pi_{m,e}^P),$$
$$\forall\, e \ne 1 \tag{29}$$

$$\pi_{m,e}^W = \hat{a}_\pi \hat{T} C_{m,e}^{B,wall} \tag{30}$$

$$\pi_{m,e}^P = \hat{a}_\pi \hat{T} C_{m,e}^{Pe} \tag{31}$$

where $\hat{a} = 2.63 \times 10^{-6}$ bar/K·ppm. The brine pressure can be calculated as follows:

$$P_{m,1}^{Be} = P_m^{IN} - \Delta P_{m,1}^B \tag{32}$$

$$P_{m,e}^{Be} = P_{m,e-1}^{Be} - \Delta P_{m,e}^B, \qquad \forall\, e \ne 1 \tag{33}$$

where $\Delta P_{m,e}^B$ is estimated from an SW RO membrane correlation given by the module producer:

$$\Delta P_{m,e}^B = 9532.4\left(\frac{F_{m,e}^{av}}{\hat{\rho}_{av}}\right)^{1.7} \tag{34}$$

$$F_{m,1}^{av} = \frac{F_m^{inem} + F_{m,1}^{Be}}{2} \tag{35}$$

$$F_{m,e}^{av} = \frac{F_{m,e-1}^{Be} + F_{m,e}^{Be}}{2}, \qquad \forall\, e \ne 1 \tag{36}$$

In turn, the flux solute $J_{m,e}^s$ is given by

$$J_{m,e}^s = \hat{b}(C_{m,e}^{B,wall} - C_{m,e}^{Pe}) \tag{37}$$

where $\hat{b}$ is the salt permeability; the membrane wall concentration is

$$C_{m,e}^{B,wall} = C_{m,e}^{Pe} + \left(\frac{C_m^{IN} + C_{m,e}^{Be}}{2} - C_{m,e}^{Pe}\right)\exp\left(\frac{V_{m,e}^w}{ks_{m,e}}\right),$$
$$e = 1 \tag{38}$$

$$C_{m,e}^{B,wall} = C_{m,e}^{Pe} + \left(\frac{C_{m,e-1}^{Be} + C_{m,e}^{Be}}{2} - C_{m,e}^{Pe}\right)\exp\left(\frac{V_{m,e}^w}{ks_{m,e}}\right),$$
$$e \ne 1 \tag{39}$$

where $ks_{m,e}$ is the mass transfer coefficient, and $V_{m,e}^w$ is the permeation velocity. These are estimated using the following expressions:

$$ks_{m,e} = 0.04 Re_{m,e}^{0.75}\widehat{Sc}^{0.33}\frac{\hat{D}}{\hat{d}_h} \tag{40}$$

$$V_{m,e}^w = \frac{J_{m,e}^w + J_{m,e}^s}{\hat{\rho}^P} \tag{41}$$

where $Re_{m,e}$, $\widehat{Sc}$, $\hat{D}$, and $\hat{d}_h$ are the Reynolds number, Schmidt number, salt diffusivity, and hydraulic diameter, respectively. They are given by

$$Re_{m,e} = \frac{\hat{d}_h U_{m,e}^s \hat{\rho}}{\hat{\mu}} \tag{42}$$

$$\widehat{Sc} = \frac{\hat{\mu}}{\hat{\rho}\hat{D}} \tag{43}$$

The superficial velocity $U_{m,e}^s$ depends on the average flow rate $F_{m,e}^{av}$, the density, and the feed cross-section open area $\hat{S}_{fc}$.

$$U_{m,e}^s = \frac{F_{m,e}^{av}}{\hat{\rho}\widehat{S}_{fc}} \tag{44}$$

Finally, the permeate concentration and flow rate are

$$C_{m,e}^{Pe} = \frac{J_{m,e}^s}{V_{m,e}^w} \times 1000 \tag{45}$$

$$F_{m,e}^{Pe} = V_{m,e}^w \hat{S}_{mem}\hat{\rho}^P \tag{46}$$

Objective Function. We minimize the total annualized cost (TAC), given by

$$\text{TAC} = \text{AOC} + \text{ccf·TCC} \tag{47}$$

where

$$\text{ccf} = \frac{(\text{ir} + 1)^{t_1}i}{(\text{ir} + 1)^{t_1} - 1}$$

In turn

$$TCC = 1.25(1.15CC_{equip}) \tag{48}$$

The equipment cost is given by

$$CC_{equip} = CC_{SWIP} + CC_{HPP} + CC_T + CC_{mem} + CC_{pv} \tag{49}$$

The salted water intake and pretreatment system cost is given by

$$CC_{SWIP} = 996(24(Q_{SW-IN}))^{0.8} \tag{50}$$

where Q_{SW-IN} is the feed flow rate to the system in m^3/h.

Costs of pump and turbines are given by the following equations:

$$CC_{HPP} = 52 \sum_p (\Delta P_p^{HPP} Q_p^{HPP}) \tag{51}$$

$$CC_{HPPR} = 52 \sum_m (\Delta P_m^{HPPR} Q_m^R) \tag{52}$$

$$CC_T = 52 \sum_t (\Delta P_t^T Q_t^T) \tag{53}$$

where ΔP_p^{HPP}, Q_p^{HPP}, ΔP_m^{HPPR}, Q_m^R, and ΔP_t^T, and Q_t^T are the pressure drops in bar and flow rates in m^3/h for the high pressure pump, recycle pump, and turbine, respectively. We note that this cost of capital is linear with power, a known shortcoming of previous models (all based on the one proposed by Malek et al.[18]) because it cannot capture the nonlinear behaviors of costs.[33] We will discuss the impact of this assumption under Results.

Other costs are as follows.

membrane module cost:

$$CC_{mem} = \sum_{m=1}^{N_{RO}} N_{pv_m} N_{em} c_{mem} \tag{54}$$

pressure vessels cost:

$$CC_{pv} = \sum_{m=1}^{N_{RO}} N_{pv_m} c_{pv} \tag{55}$$

annual operational costs:

$$AOC = OC_{lab} + OC_{chem} + OC_m + OC_{memr} + OC_{ins} + OC_{pow} \tag{56}$$

labor cost:

$$OC_{lab} = c_{lab} Q_P t_a \tag{57}$$

where the permeate production rate Q_P and the annual operational time t_a are used.

cost of chemicals:

$$OC_{chem} = 0.018 Q_{SW-IN} t_a \tag{58}$$

cost for replacement and maintenance:

$$OC_m = 0.01 TCC \tag{59}$$

membrane replacement cost:

$$OC_{memr} = 0.2 CC_{mem} \tag{60}$$

insurance costs:

$$OC_{ins} = 0.005 TCC \tag{61}$$

electric energy costs:

$$OC_{pow} = C_{en}(PP_{SWIP} + PP_{RO})t_a \tag{62}$$

The energy consumed for intake and pretreatment system is given by

$$PP_{SWIP} = \frac{1}{36} \frac{Q_{SW-IN} \Delta \hat{P}_{SWIP}}{\hat{\eta}_{SWIP}} \tag{63}$$

Electric energy consumed by the reverse osmosis plant is given by

$$PP_{RO} = \frac{1}{36} \left(\sum_p \frac{\Delta P_p^{HPP} Q_p^{HPP}}{\hat{\eta}_{HPP}} + \sum_m \frac{\Delta P_m^{HPPR} Q_m^R}{\hat{\eta}_{HPPR}} - \sum_t \Delta P_t^T Q_t^T \hat{\eta}_T \right) \tag{64}$$

3. METAMODELS

We use simple quadratic polynomials as metamodels. The equations of the membrane diffusion model were solved numerically for different inlet conditions (values selected according to the bounds of the problem) to obtain a mesh of input−output data pairs. We identified two different regions for the permeate concentration: a *linear region* and a *nonlinear region*. The expressions are presented next.

Linear Region. The concentration was adjusted to a first-order polynomial as follows:

$$C^{Pe} = K_1 + K_2 P^{IN} + K_3 C^{IN} + K_4 F^{IN} \tag{65}$$

Nonlinear Region. The permeate concentration was adjusted to a second-order polynomial:

$$\begin{aligned} C^{Pe} = &K_1 + K_2(P^{IN})^2 + K_3(C^{IN})^2 + K_4(F^{IN})^2 + K_5 P^{IN} \\ &+ K_6 C^{IN} + K_7 F_{m,e}^{in} + K_8(P^{IN})^2(C^{IN})^2 + K_9(P^{IN})^2(F^{IN})^2 \\ &+ K_{10}(C^{IN})^2(F^{IN})^2 + K_{11}(P^{IN})^2(C^{IN})^2(F^{IN})^2 + K_{12}P^{IN} \\ &C^{IN} + K_{13}P^{IN}F^{IN} + K_{14}C^{IN}F^{IN} \\ &+ K_{15}P^{IN}C^{IN}F^{IN} \end{aligned} \tag{66}$$

The permeate flow was adjusted to a first-order polynomial for all of the operation region:

$$\begin{aligned} F^{Pe} = &K_1 + K_2 P^{IN} + K_3 C^{IN} + K_4 F^{IN} + K_5 P^{IN} C^{IN} \\ &+ K_6 P^{IN} F^{IN} + K_7 C^{IN} F^{IN} + K_8 P^{IN} C^{IN} F^{IN} \end{aligned} \tag{67}$$

To obtain the coefficients of the metamodels we used a diploid genetic algorithm (DGA) programmed in MATLAB.[34] The code follows the description given by Fonteix et al.[35] The method tends to imitate principles of organic evolution processes as rules for an optimization procedure; this is based in genetic concepts such as population, recombination, and mutation as evolution rules to guide the optimum search. The simulations were developed on a laptop computer with an Intel Core i7-3610QM CPU@2.3 GHz (8 CPUs) processor with 8192 MB of RAM. Each variable (C^{Pe}, F^{Pe}), was evaluated using eqs 65−67 for different inlet conditions (P^{IN}, C^{IN}, and

F^{IN}) using estimated coefficients, to generate the metamodel solutions mesh. The same inlet conditions were used with eqs 27–46 to generate the rigorous solutions mesh. The fitness function that was minimized to obtain the coefficients is the following:

$$F_{\text{obj}} = \sum_i^N (V^{\text{rig.}} - V^{\text{met.}})^2 \tag{68}$$

where V is the variable to be adjusted (C^{Pe}, F^{Pe}), N is the total number of points, and the superscripts "rig." and "met." represent the values obtained from the rigorous method and the metamodel prediction, respectively. The Supporting Information shows additional details of the metamodel.

4. SOLUTION STRATEGY

We tested three different solution strategies.

(a) A genetic algorithm (1000 individuals, 10 generations, 100 survivors, and 100 mutants) using the rigorous equations and the metamodel equations as well was tested. The GA has four random variables per stage: flow entering each pressure vessel, pressure entering all pressure vessels, the number of modules in each stage, and the recycling ratio. Once these are fixed for each individual of the population (1000), the respective model is solved calculating first the sequence of membrane models using the transport phenomenon equations or the metamodel expressions according to the case, and then the recycle is calculated and the stage is recalculated based on the new inlet conditions of flow and concentration until convergence. The rest is the classical setup of a diploid GA algorithm. We considered the rigorous model and the linear and nonlinear metamodels depending on the regions where they are the most accurate. Indeed, we used the linear model when the ratio between inlet concentration and inlet pressure was lower than 950 and the nonlinear model when this ratio was equal to or greater than 950; this boundary ratio was obtained from the model adjustment for different inlet flows.

(b) A rigorous MINLP composed of the mass balances (eqs 1–11), the reverse stages model (eqs 12–26), the membrane transport phenomenon (diffusion) model (eqs 27–46), and the economic model (eqs 48–64) was solved with DICOPT[36] programmed in GAMS[37] using the results obtained from the genetic algorithm as initial values. In particular, the MINLP is solved considering the number of pressure vessels (N_{pv}) as a continuous variable and then is rerun fixing the N_{pv} to the nearest integer value.

(c) Some global optimization solvers were used for the same rigorous MINLP model previously presented in (b): Baron,[38] Antigone,[39] and Rysia.[40] The first two are commercial and the latter is not, but has proved to solve certain problems that the aforementioned two cannot solve.

5. RESULTS

The data for the modules are presented in Table 1, and the economic parameters are presented in Table 2. Table 3 shows the optimization results for the RO system for a targeted permeate concentration of 500 ppm and a flow rate of 100 kg/s, with an inlet water concentration of 35 000 ppm. We also set a maximum of 87 000 ppm for the brine concentration, a reasonable value before scaling onset. The necessary parameters to describe the diploid GA[35] used were 1000 individuals, 10 generations, 100 survivors, 100 mutants, and a mutation rate equal to 0.01. In Table 3 we report the final

Table 1. Reverse Osmosis Module Parameters

parameter	value
effective area, S_{mem} (m^2)	35.33
water permeability, A (kg/m^2·s·bar)	2.4×10^{-4}
salt permeability, B (kg/m^2·s)	2×10^{-5}
diffusivity coefficient, D (m^2/s)	1.35×10^{-9}
hydraulic diameter, d_{h} (m)	9.35×10^{-4}
feed cross-section open area, S_{fc} (m^2)	0.0147
maximum inlet flow rate, F^{maxin} (kg/s)	5
minimum inlet flow rate, F^{minin} (kg/s)	1

Table 2. Economic Parameters

parameter	value
capital charge factor, ccf	0.088
membrane unitary cost, C_{mem} (USD)	750
pressure vessel unitary cost, C_{pv_m} (USD)	1000
labor cost factor, c_{lab} (USD)	0.05
annual operational time, t_{a} (h/year)	8000
pressure difference for intake, ΔP_{SWIP} (bar)	5
energy price, C_{en} ($/kWh)	0.05
intake pump efficiency, η_{SWIP}	0.75
high pressure pump efficiency, η_{SWIP}	0.75
turbine efficiency, η_{SWIP}	0.75

number of vessels obtained, considering it as a continuous value and, in the case of the MINLP, we report both the continuous value obtained and the fixed value used for the final MINLP run (in parentheses). The TAC reported for the MINLP is based on the integer value of the number of vessels. The optimization renders the flow of the brine and the inlet flow needed.

The rigorous MINLP models using the results from the GAs as a starting point give the same result with slightly different solution times (5.7 s for using the initial values from the GA run using the metamodel versus 6.8 s using the initial values from the GA run with the rigorous model). We note that the genetic algorithm using the rigorous model was disproportionally time-consuming (280 h vs 20 min). The time-consuming step is the iterative solution of the nonlinear set of equations. The fitness (TAC) of each individual of the population at each GA iteration is evaluated by solving the membrane module equations (eqs 27–46). This is done as follows: The total inlet flow and the inlet concentration are known from the problem specification and then eqs 27–46 are solved to obtain permeate flow and concentration; the brine flow and concentration are calculated from the mass balance. We remind the reader that the Matlab "solve" feature is used in this step, of which we have little detailed information. These values are then used as the inlet conditions for the next module. Once the last module is solved, the concentration of the recycle is known and one can start at the first module again upon convergence. Each solution of eqs 27–46 takes for a single membrane module 5–60 s to be solved, and a single stage takes about 10 iterations to converge. We thus explain the large computing time when we realize that we use 1000 individuals and 10 generations. Conversely, the metamodel does not need to iterate to solve the same module equations.

Table 3 presents the TAC for the rigorous MINLP fixing the number of pressure vessels N_{pv} to the nearest integer values obtained from the rigorous MINLP (considering N_{pv} as continuous). The TAC values differ only in 0.00033%,

Table 3. Optimization Results[a]

	genetic algorithm using metamodel		genetic algorithm using rigorous model		rigorous MINLP	
TAC ($)	1,796,169		1,806,500		1,781,499	
stage	S1	S2	S1	S1	S1	S2
inlet pressure (bar)	73	80	67.6	79.9	63	79.4
salted water flow (kg/s)	167.65		167.65		166.57	
each pressure vessel inlet flow (kg/s)	3.5	3.5	2.14	3.47	2.6	2.59
no. of modules	8	8	8	8	8	8
no. of pressure vessels as continuous variable (as integer)	47.9	25.4	78.3	24.5	63.6 (64)	37.2 (37)
flow recycle 1 (kg/s)	0		0		0	
flow recycle 2 (kg/s)	0		0		0	
computing time	∼20 min		280 h		5.5 s	

[a]Permeate concentration, 500 ppm; permeate flow rate, 100 kg/s; inlet water concentration, 35 000 ppm.

Table 4. Optimal Solutions for Different Scenarios[a]

	feed seawater concentration (ppm)											
	30 000				40 000				50 000			
	GA with metamodel		rigorous MINLP		GA with metamodel		rigorous MINLP		GA with metamodel		rigorous MINLP	
TAC ($)	4,723,835		4,700,784		2,582,401		2,629,873		532,703		551,140	
stage	S1	S2	S1	S2	S1	S2	S1	S2	S1	S2	S1	S2
inlet pressure (bar)	78.4	80	55.8	73.5	73.4	78.8	65.9	75.3	75.4	77.6	78.1	76.8
salted water flow (kg/s)	450		450		250		250		50		50	
permeate flow (kg/s)	296.5		296.5		135.8		135.8		21.38		21.38	
pressure vessel inlet flow (kg/s)	4.0	4.0	1.8	1.5	4.0	4.0	2.4	2.1	4.0	4.0	2.5	2.7
no. of modules	8	8	8	8	7	8	7	8	5	7	5	7
no. of pressure vessels as continuous variable (as integer)	112.5	52.9	245.6 (246)	155.6 (156)	62.6	38.2	103.6 (104)	73.9 (74)	12.5	9.0	19.6 (20)	12.8 (13)
flow recycle 1 (kg/s)	0		0		0		0		0		0	
flow recycle 2 (kg/s)	0		0		0		0		0		0	
computing time	∼20 min		4.2 s		∼22 min		5.1 s		∼24 min		4.7 s	

[a]Permeate maximum concentration, 500 ppm.

indicating that the approximation does not introduce a significant error.

Because we made several runs using the GA with the metamodel followed by the rigorous MINLP (as detailed below), finding similar times (less than 30 min), we are confident that the pattern will repeat for other cases and/or with other parameter data.

The rigorous MINLP was also run without initial values in DICOPT[36] and Antigone,[39] and we did not obtain a feasible solution. When trying Baron,[38] after a predefined time limit of 250 h, the solver finished without attaining convergence, with the relative gap at 18.72%. We also ran Baron[38] fixing the binary variables for the number of membrane modules and we did not obtain a feasible solution.

In an attempt to implement Rysia,[40] we developed a relaxed version (linear lower bound) of the rigorous MINLP. Although the rational terms of the model can be reformulated to render a bilinear model, the presence of exponential terms made us select a different approach, which is the use of images of monotonic functions in each domain variable's partition, as it was performed in several papers[41−44] that follow the one introducing Rysia.[40] When running Rysia, the upper bound is the rigorous MINLP and Rysia is run using the results from the lower bound as initial values. Before trying bound contraction, we attempted to increase the number of partitions in the lower bound to see if the gap at the root node can be reduced. The result is that we reached a region where there is no improvement in the objective value when the number of intervals for the partitioned variables was increased. For example, when we run with 2, 4, 8, and 10 intervals to partition the decision variables, we obtain a sequence of slowly increasing lower bound values ($1,293,594, $1,318,176, $1,528,365, and $1,540,456) at elevated computational costs of 0.1, 1.3, 6.0, and 10 h, respectively. In the meantime, the upper bound rendered an optimum with an objective of $1,814,528, which is only 1.8% larger than the optimum identified in Table 3. Clearly, an increase of the number of intervals leads to unacceptable computing times. When bound contraction was attempted using two intervals, none of the bounds for the partitioned variables could be contracted. We did not try the bound contraction procedure using three intervals, since the computational cost is already high, because the procedure is iterative and needs to be implemented for each one of the 84 partitioned variables each time. Each run takes 30 min, so it will take about 42 h to complete the first iteration, and we are not sure that it will take just one pass.

All the above results show that the nonlinearity of the RON−MINLP model presents important convergence diffi-

culties, and is computationally expensive, especially if good initial values are unknown for local solvers. While we cannot explain the reasons why Baron and Antigone fail, in the case of Rysia, we can only say that it should be able to solve the problem with enough number of partitions, if it were not for the computational effort involved. Thus, for the rest of this paper, we will use a genetic algorithm using metamodels to initialize a rigorous MINLP model.

The results for different inlet water concentrations and different target permeate flows and a permeate concentration of 500 ppm are shown, for two stages, in Table 4. We note that, in this case, we no longer fix the permeate flow; instead the inlet flow is fixed maintaining a maximum brine concentration of 87 000 ppm.

Results presented in Tables 3 and 4 do not show a brine recycle flow, despite that recycling helps in reducing concentration polarization (increasing the velocity through the membrane module). Optimal solutions avoid it because of the recycle pumps (HPPR) needed to compensate the pressure drop of the membrane module, thus increasing the total capital cost and power consumption since they are high-pressure pumps. Incidentally, brine recycle also increases the system salt passage leading to unacceptable salt permeate concentrations in some cases.[45]

The main differences in the operation conditions (decision variables) between the genetic algorithms using the metamodel and the rigorous MINLP (Tables 3 and 4) are associated with the precision of the metamodel, which underestimates some values of the operating variables in the region closer to the bounds. Thus, although the genetic metamodel is not completely suitable to determine operating conditions, it produces good initial estimates as starting points for the rigorous MINLP.

We now turn to an analysis of the effect of the feed flow and the salt concentration in the feed on the total annualized cost. Figure 4 presents the rigorous solution obtained for a feed flow
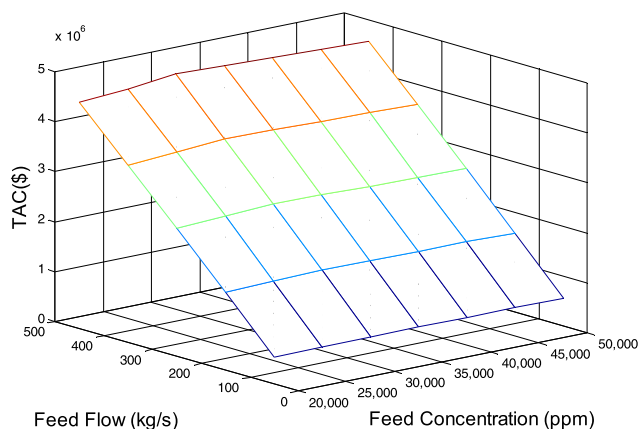
For a fixed flow the differences in the extremes are −3.6% (cost for 20 000 ppm vs cost of 30 000 ppm) and −2.6% (cost for 50 000 ppm vs cost of 30 000 ppm). For a feed concentration of 30 000 ppm and larger, the TAC does not change significantly because the requirements for a larger pump power are compensated by less membrane area due to higher concentrations. On the other side, for feed concentrations of 20 000 and 25 000 ppm the reduction is due to the use of membrane module with high retention parameters for seawater, while these concentrations are more related to brackish water concentrations. The reduction in TAC here is due to smaller pumping needs driven by lower concentrations.

Such small differences in TAC for a large range of feed concentrations lead us to conclude that an average TAC for each flow is a good representation of all.

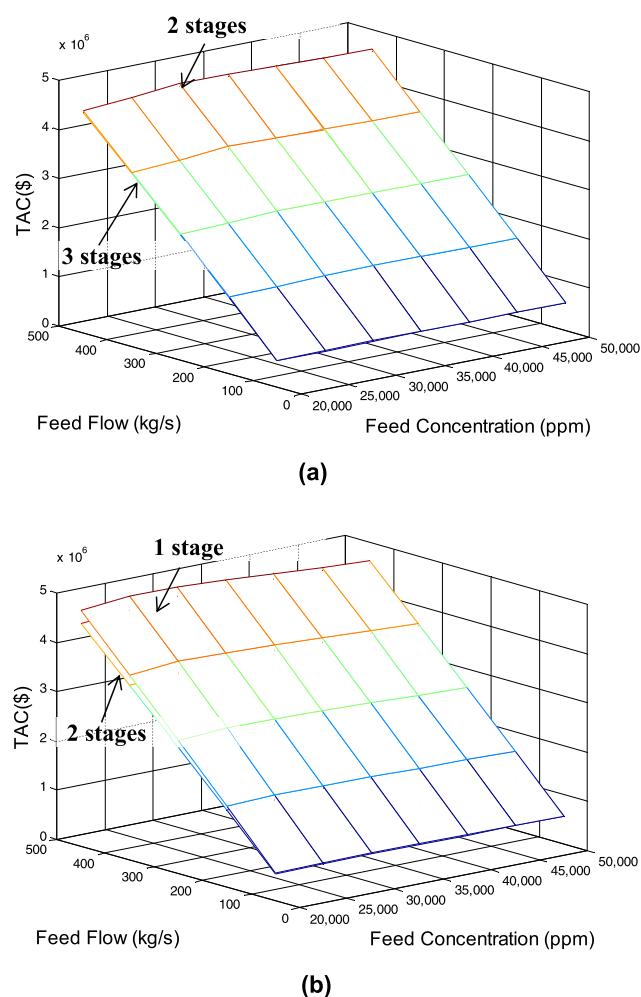We now explore the influence of the number of RO stages. The results are presented in Figure 5. The maximum TAC

(a)

(b)

Figure 5. Effect of number of stages: (a) two vs three stages; (b) one vs two stages.

Figure 4. TAC for different inlet flows and seawater concentrations (two stages).

between 50 and 450 kg/s and a feed salt concentration between 20 000 and 50 000 ppm and running the GA with the metamodel, followed by the rigorous MINLP solved using DICOPT with initial values obtained from the GA.

The results show that the TAC presents two regions with an apparent maximum at 30 000 ppm of feed concentration. We cannot say for sure that the maximum is exactly at 30 000 ppm, given the discrete nature of the number of points investigated.

difference between three stages and two stages is about 1.6% (Figure 5a); although it is not noticeable in the figure, the surfaces have a transition point from constant TAC to monotonic TAC at 30 000 ppm, as explained above. The TAC values for two stages are lower than those for three stages for feed concentrations of 40 000 ppm and larger. For feed concentrations of 35 000 ppm and lower the design for three

stages is lower in cost than that for two stages, again barely noticeable in Figure 5a. This behavior is obtained using linear cost for pumps as a function of power (eqs 51−53). One would argue that the use of a power law for cost, with other exponents, might change the results. Indeed, Lu et al.[22] and Kim et al.[14] used a power law with an exponent of 0.96 and the general literature on costs suggests values as low as 0.5. We tested the model for various points using 0.96, 0.7, and 0.5. The results are always the same: for every flow rate, the region where three stages are of lower cost than two stages is for every flow below 35 000 ppm. For 40 000 ppm and above, two stages are cheaper than three. This is consistent with the fact that at higher concentrations the power is constant because the pressure has reached its maximum. Thus, two pumps makes more sense than three pumps in that region. Below 40 000 ppm, more pumps are compensated by a smaller number of membrane modules (lower membrane area). The extreme differences (cost of three stages vs cost of two stages) are −1.59 and +5.97% for $n = 0.96$, −3.38 and +18.30% for $n = 0.7$, and −3.51 and +19.25% for $n = 0.5$. These are big differences and are a warning about the cost functions that need to be used.

In turn, the optimal TAC results for one stage are larger than those for two stages with a maximum difference close to 7% (Figure 5b).

When analyzing the results, there were solutions that used the maximum membrane modules allowed in a pressure vessel according to the fabricant, especially those corresponding to 35 000 ppm or lower. Therefore, a new set of solutions was obtained allowing the variable to use up 16 membrane modules. In this case, we found solutions using up to 14 membrane modules. These results are presented in Figure 6.
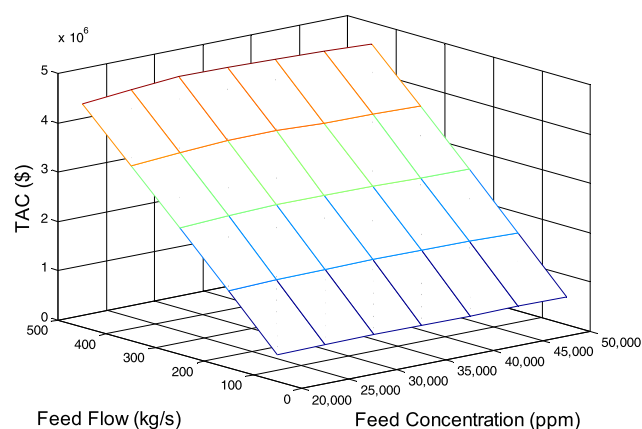

Figure 6. TAC for different inlet flows and seawater concentrations. Maximum number of membrane modules (N_e^{max}) equal to 16.

The maximum difference between the use of a maximum of 8 modules and the use of a maximum of 16 modules was lower than 0.7% (indistinguishable in Figure 6), so there is no improvement in using a larger number of membrane modules per vessel. This behavior is explained because an increase in the maximum membrane modules is compensated with variations on the inlet stage conditions (pressure and pressure vessel inlet flow F_m^{inem}), but these variations have no significant effect on the TAC. We can conclude that the model is rather insensitive to the number of modules and that also perhaps explains the convergence difficulties.

All the above results represent optimal values obtained minimizing the TAC for a fixed concentration and flow rate of the permeate (Table 3) or flow rate of the feed (rest of results). We now investigate the minimization of the cost per unit of fresh water produced with a fixed targeted concentration. Results are shown in Figure 7. We observed a
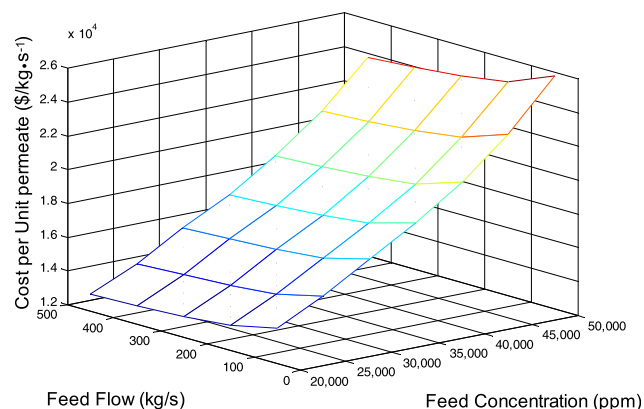

Figure 7. Optimal TAC per unit permeate flow. Concentration of permeate, 500 ppm.

sensibility to the feed concentration and the feed flow, different from the one observed in Figure 4. In the case of Figure 4, for a fixed permeate concentration of 500 ppm, the TAC is not significantly affected by the change in the feed concentration when the feed is maintained constant. However, when the inlet concentration varies, the amount of permeate flow decreases with feed concentration (shown in Figure 8). Since the TAC
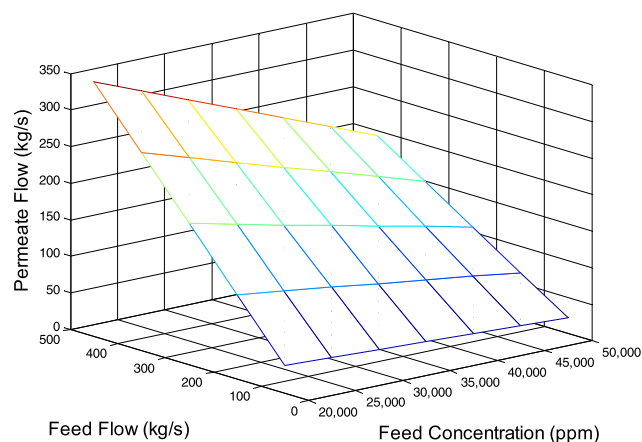

Figure 8. Permeate flow (two stages, 500 ppm permeate).

values for both figures (Figures 4 and 7) are the same but the amount of obtained fresh water varies with the inlet concentration, the cost per unit of produce fresh waters increases with the feed concentration.

6. CONCLUSIONS

A new methodology to solve a nonlinear mathematical model for the optimal design of RO is proposed. Metamodels were used to reduce the mathematical complexity and get accurate solutions using a genetic algorithm. Then, the results were used as initial values to solve the full nonlinear model using GAMS/DICOPT. This allows getting optimal solutions for a complex MINLP problem with less computational effort. One of the

major advances of our approach is that initial values are not needed (always a problem for practitioners using MINLP codes), as the GA provides them.

The total annualized cost increases with an increase in the feed flow and presents little variations for different feed salt concentrations at a fixed inlet flow, indicating that a reverse osmosis plant could have adaptation capability for variations in the inlet concentration without major effects on the TAC.

The effect of the number of stages was studied for different feed flows and seawater concentrations, finding that one stage has the largest TAC and the differences between two and three stages are small, but dependent on the costing of pumps used.

The effect of the number of membrane modules in a pressure vessel was also investigated, finding that increasing the maximum number of membranes allowed in a commercial pressure vessel does not have any advantage over the TAC values obtained.

■ ASSOCIATED CONTENT

ⓢ Supporting Information

The Supporting Information is available free of charge on the ACS Publications website at DOI: 10.1021/acs.iecr.8b02639.

Metamodel adjustment, operational region, set of constants for the linear and nonlinear regions, influence of decision variables (PDF)

■ AUTHOR INFORMATION

Corresponding Author

*E-mail: bagajewicz@ou.edu.

ORCID Ⓞ

Mario Noriega: 0000-0003-2876-702X

Miguel Bagajewicz: 0000-0003-2195-0833

Notes

The authors declare no competing financial interest.

■ NOMENCLATURE

AOC = annual operational cost [$]
C = salt concentration [ppm]
$C^{B,wall}$ = membrane wall concentration [ppm]
C_P^{max} = maximum permeate concentration [ppm]
CC_{equip} = total equipment cost [$]
ccf = capital charge factor
CC_{HPP} = high pressure pump cost [$]
CC_{mem} = membrane module cost [$]
c_{lab} = labor cost factor [$]
C_{en} = electricity cost [$/(kWh)]
c_{mem} = membrane module unitary cost [$]
CC_{pv} = total pressure vessel cost [$]
c_{pv} = unitary pressure vessel cost [$]
CC_{SWIP} = seawater intake and pretreatment system cost [$]
CC_T = turbine cost [$]
F = flow rate [kg/s]
F^{av} = average flow rate [kg/s]
F_R = recycle flow rate [kg/s]
J^s = solute flux [kg/(s·m^2)]
J^w = water flux [kg/(s·m^2)]
ir = annual interest rate
ks = mass transfer coefficient [m/s]
N_e = number of membrane modules per pressure vessel
N_{pv} = number of pressure vessels of stage m
N_{RO} = number of reverse osmosis stages

OC_{chem} = cost of chemicals [$]
OC_{ins} = insurance costs [$]
OC_{lab} = labor cost [$]
OC_{pow} = electric energy costs [$]
OC_m = cost for replacement and maintenance [$]
OC_{memr} = membrane replacement cost [$]
P = pressure [bar]
PP_{SWIP} = energy consumed for intake and pretreatment system [kWh]
PP_{RO} = electric energy consumed by the reverse osmosis plant [kWh]
Q = flow rate [m^3/h]
Q_R = recycle flow rate [m^3/h]
Q_{SW-IN} = feed flow rate to the system [m^3/h]
Re = Reynolds number
Sc = Schmidt number
TAC = total annualized cost [$]
TCC = total capital cost [$]
U^s = superficial velocity [m/s]
V^w = permeation velocity [m/s]
y = binary variable
t_a = annual operation time [h]
t_1 = lifetime of the plant [years]
ΔP^B = brine side pressure difference [bar]
ΔP^{nd} = net driving pressure difference [bar]
ΔP = pressure difference [bar]

Parameters

$\hat{a}$ = pure water permeability [kg/(s·m^2·bar)]
$\hat{a}_\pi$ = van't Hoff constant [bar/(K·ppm)]
$\hat{b}$ = salt permeability [kg/(s·m^2)]
$\hat{D}$ = salt diffusivity [m^2/s]
$\hat{d}_h$ = hydraulic diameter [m]
$\hat{P}^{Pe}$ = permeate outlet pressure [bar]
$\hat{T}$ = inlet temperature [K]
$\hat{S}_{fc}$ = feed cross-section open area [m^2]
$\hat{S}_{mem}$ = active membrane area [m^2]
$\Delta \hat{P}_{SWIP}$ = seawater intake pressure difference [bar]

Superscripts

av = average
B = brine
Be = brine current of module e from stage m
B$-$F$_{BO}$ = interconnection between brine and brine final discharge
HPP = high pressure pump
HPPR = recycle high pressure pump
IN = inlet
inem = inlet of first modules of stage m
O = outlet
P = permeate
Pe = permeate current of module e from the stage m
RO = reverse osmosis
T = turbine
T$-$F$_{BO}$ = interconnection between turbine and brine final discharge
W = membrane wall

Subscripts

BO = brine final discharge
e = membrane module e
m = RO stage m
p = pump p
pv = pressure vessel
PO = permeate final current

S = feed current

SWIP = seawater intake and pretreatment

t = turbine t

Greek Symbols

$\hat{\rho}$ = density $[kg/m^3]$

$\hat{\mu}$ = dynamic viscosity $[kg/m \cdot s]$

η = efficiency

π = osmotic pressure $[bar]$

■ REFERENCES

(1) Kucera, J. *Desalination: Water from Water*, 1st ed.; John Wiley and Sons: 2014.

(2) Ghaffour, N.; Bundschuh, J.; Mahmoudi, H.; Goosen, M. F. A. Renewable Energy-Driven Desalination Technologies: A Comprehensive Review on Challenges and Potential Applications of Integrated Systems. *Desalination* **2015**, *356*, 94−114.

(3) Ghobeity, A.; Mitsos, A. Optimal Design and Operation of Desalination Systems : New Challenges and Recent Advances. *Curr. Opin. Chem. Eng.* **2014**, *6*, 61−68.

(4) Choi, J. S.; Kim, J. T. Modeling of Full-Scale Reverse Osmosis Desalination System: Influence of Operational Parameters. *J. Ind. Eng. Chem.* **2015**, *21*, 261−268.

(5) Evangelista, F. A. Short Cut Method for the Design of Reverse Osmosis Desalination Plants. *Ind. Eng. Chem. Process Des. Dev.* **1985**, *24*, 211−223.

(6) Zhu, M.; El-Halwagi, M. M.; Al-Ahmad, M. Optimal Design and Scheduling of Flexible Reverse Osmosis Networks. *J. Membr. Sci.* **1997**, *129*, 161−174.

(7) Voros, N.; Maroulis, Z. B.; Marinos-Kouris, D. Optimization of Reverse Osmosis Networks for Seawater Desalination. *Comput. Chem. Eng.* **1996**, *20*, S345−S350.

(8) Voros, N. G.; Maroulis, Z. B.; Marinos-Kouris, D. Short-Cut Structural Design of Reverse Osmosis Desalination Plants. *J. Membr. Sci.* **1997**, *127*, 47−68.

(9) Maskan, F.; Wiley, D. E.; Johnston, L. P. M.; Clements, D. J. Optimal Design of Reverse Osmosis Module Networks. *AIChE J.* **2000**, *46* (5), 946−954.

(10) Marcovecchio, M. G.; Aguirre, P. a.; Scenna, N. J. Global Optimal Design of Reverse Osmosis Networks for Seawater Desalination: Modeling and Algorithm. *Desalination* **2005**, *184* (1−3), 259−271.

(11) Geraldes, V.; Pereira, N. E.; Norberta de Pinho, M. Simulation and Optimization of Medium-Sized Seawater Reverse Osmosis Processes with Spiral-Wound Modules. *Ind. Eng. Chem. Res.* **2005**, *44*, 1897−1905.

(12) Lu, Y. Y.; Hu, Y. D.; Zhang, X. L.; Wu, L. Y.; Liu, Q. Z. Optimum Design of Reverse Osmosis System under Different Feed Concentration and Product Specification. *J. Membr. Sci.* **2007**, *287* (2), 219−229.

(13) Vince, F.; Marechal, F.; Aoustin, E.; Bréant, P. Multi-Objective Optimization of RO Desalination Plants. *Desalination* **2008**, *222* (1−3), 96−118.

(14) Kim, Y. S. Y. M.; Kim, S. J.; Kim, Y. S. Y. M.; Lee, S.; Kim, I. S.; Kim, J. H. Overview of Systems Engineering Approaches for a Large-Scale Seawater Desalination Plant with a Reverse Osmosis Network. *Desalination* **2009**, *238* (1−3), 312−332.

(15) Oh, H. J.; Hwang, T. M.; Lee, S. A Simplified Simulation Model of RO Systems for Seawater Desalination. *Desalination* **2009**, *238* (1−3), 128−139.

(16) Al-Bastaki, N. M.; Abbas, A. Predicting the Performance of RO Membranes. *Desalination* **2000**, *132* (1−3), 181−187.

(17) Wang, J.; Dlamini, D. S.; Mishra, A. K.; Pendergast, M. T. M.; Wong, M. C. Y.; Mamba, B. B.; Freger, V.; Verliefde, A. R. D.; Hoek, E. M. V. A Critical Review of Transport through Osmotic Membranes. *J. Membr. Sci.* **2014**, *454*, 516−537.

(18) Malek, A.; Hawlader, M. N. A.; Ho, J. C. Design and Economics of RO Seawater Desalination. *Desalination* **1996**, *105* (3), 245−261.

(19) Du, Y.; Xie, L.; Wang, Y.; Xu, Y.; Wang, S. Optimization of Reverse Osmosis Networks with Spiral-Wound Modules. *Ind. Eng. Chem. Res.* **2012**, *51*, 11764−11777.

(20) Sassi, K. M.; Mujtaba, I. M. Effective Design of Reverse Osmosis Based Desalination Process Considering Wide Range of Salinity and Seawater Temperature. *Desalination* **2012**, *306*, 8−16.

(21) Alnouri, S. Y.; Linke, P. A Systematic Approach to Optimal Membrane Network Synthesis for Seawater Desalination. *J. Membr. Sci.* **2012**, *417−418*, 96−112.

(22) Lu, Y.; Liao, A.; Hu, Y. Design of Reverse Osmosis Networks for Multiple Freshwater Production. *Korean J. Chem. Eng.* **2013**, *30* (5), 988−996.

(23) Skiborowski, M.; Mhamdi, A.; Kraemer, K.; Marquardt, W. Model-Based Structural Optimization of Seawater Desalination Plants. *Desalination* **2012**, *292*, 30−44.

(24) Kleijnen, J. P. C. Regression and Kriging Metamodels with Their Experimental Designs in Simulation . *A Review* **2017**, *256*, 1−16.

(25) Mahmoudi, S.; Trivaudey, F.; Bouhaddi, N. Benefits of Metamodel-Reduction for Nonlinear Dynamic Response Analysis of Damaged Composite Structures. *Finite Elem. Anal. Des.* **2016**, *119*, 1−14.

(26) Kaminski, B. Interval Metamodels for the Analysis of Simulation Input−Output Relations. *Simul. Modell. Pract. Theory* **2015**, *54*, 86−100.

(27) Wen, J.; Yang, H.; Jian, G.; Tong, X.; Li, K.; Wang, S. International Journal of Heat and Mass Transfer Energy and Cost Optimization of Shell and Tube Heat Exchanger with Helical Baffles Using Kriging Metamodel Based on MOGA. *Int. J. Heat Mass Transfer* **2016**, *98*, 29−39.

(28) Psaltis, A.; Sinoquet, D.; Pagot, A. Systematic Optimization Methodology for Heat Exchanger Network and Simultaneous Process Design. *Comput. Chem. Eng.* **2016**, *95*, 146−160.

(29) Broad, D. R.; Dandy, G. C.; Maier, H. R. Environmental Modelling & Software A Systematic Approach to Determining Metamodel Scope for Risk- Based Optimization and Its Application to Water Distribution System. *Environ. Model. Softw.* **2015**, *69*, 382−395.

(30) Beh, E. H. Y.; Zheng, F.; Dandy, G. C.; Maier, H. R.; Kapelan, Z. Environmental Modelling & Software Robust Optimization of Water Infrastructure Planning under Deep Uncertainty Using Metamodels. *Environ. Model. Softw.* **2017**, *93*, 92−105.

(31) Bucher, C. Metamodels of Optimal Quality for Stochastic Structural Optimization. *Probabilistic Eng. Mech.* **2018**, *54*, 131−137.

(32) Jaffal, I.; Inard, C. A Metamodel for Building Energy Performance. *Energy Build* **2017**, *151*, 501−510.

(33) Guthrie, K. M. Data and Techniques for Preilinary Capital Cost Estimation. *Chem. Eng.* **1969**, *24*, 114−142.

(34) The Mathworks Inc. *MATLAB*; MathWorks: http://www.mathworks.com/products/matlab/.

(35) Fonteix, C.; Bicking, F.; Perrin, E.; Marc, I. Haploid and Diploid Algorithms, a New Approach for Global Optimization: Compared Performances. *Int. J. Syst. Sci.* **1995**, *26* (10), 1919−1933.

(36) Grossmann, I.; Viswanathan, J.; Vecchietti, A.; Raman, R.; Kalvelagen, E. *DICOPT*; GAMS: https://www.gams.com/.

(37) Rosenthal, R. E. *GAMS — A User's Guide*; GAMS: 2015.

(38) Sahinidis, N. V. BARON: A General Purpose Global Optimization Software Package. *J. Glob. Optim.* **1996**, *8* (2), 201−205.

(39) Misener, R.; Floudas, C. A. ANTIGONE: Algorithms for Continuous/Integer Global Optimization of Nonlinear Equations. *J. Glob. Optim.* **2014**, *59* (2−3), 503−526.

(40) Faria, C.; Bagajewicz, M. J. A New Approach for Global Optimization of a Class of MINLP Problems with Applications to Water Management and Pooling Problems. *AIChE J.* **2012**, *58* (8), 2320−2335.

(41) Carvalho, M.; Secchi, A. R.; Bagajewicz, M. Model Reformulation and Global Optimization of Oil Production Using Gas Lift. *Ind. Eng. Chem. Res.* **2016**, *55* (38), 10114−10120.

(42) Kim, S. Y.; Bagajewicz, M. Global Optimization of Heat Exchanger Networks Using a New Generalized Superstructure. *Chem. Eng. Sci.* **2016**, *147*, 30−46.

(43) Kim, S. Y.; Jongsuwat, P.; Suriyapraphadilok, U.; Bagajewicz, M. Global Optimization of Heat Exchanger Networks. Part 1: Stages/Substages Superstructure. *Ind. Eng. Chem. Res.* **2017**, *56* (20), 5944−5957.

(44) Kim, S. Y.; Bagajewicz, M. Global Optimization of Heat Exchanger Networks. Part 2: Stages/Substages Superstructure with Variable Cp. *Ind. Eng. Chem. Res.* **2017**, *56* (20), 5958−5969.

(45) Dow Water & Process Solutions. *FILMTEC^{TM} Reverse Osmosis Membranes: Technical Manual*; Form No. 609-00071-1009; Dow Chemical Co.: 2011.